Explicit Symplectic Geometric Algorithms for Quaternion Kinematical Differential Equation

Hong-Yan Zhang, Zi-Hao Wang, Lu-Sha Zhou, Qian-Nan Xue, Long Ma, and Yi-Fan Niu

***Abstract*—Solving quaternion kinematical differential equations (QKDE) is one of the most significant problems in the automation, navigation, aerospace and aeronautics literatures. Most existing approaches for this problem neither preserve the norm of quaternions nor avoid errors accumulated in the sense of long term time. We present explicit symplectic geometric algorithms to deal with the quaternion kinematical differential equation by modelling its time-invariant and time-varying versions with Hamiltonian systems and adopting a three-step strategy. Firstly, a generalized Euler's formula and Cayley-Euler formula are proved and used to construct symplectic single-step transition operators via the centered implicit Euler scheme for autonomous Hamiltonian system. Secondly, the symplecticity, orthogonality and invertibility of the symplectic transition operators are proved rigorously. Finally, the explicit symplectic geometric algorithm for the time-varying quaternion kinematical differential equation, i.e., a non-autonomous and non-linear Hamiltonian system essentially, is designed with the theorems proved. Our novel algorithms have simple structures, linear time complexity and constant space complexity of computation. The correctness and efficiencies of the proposed algorithms are verified and validated via numerical simulations.**

***Index Terms*—Linear time-varying system, navigation system, quaternion kinematical differential equation (QKDE), real-time computation, symplectic method.**

I. Introduction

QUATERNIONS, invented by the Irish mathematician W. R. Hamilton in 1843, have been extensively utilized in physics [1], [2] aerospace and aeronautical technologies [3]−[12], robotics and automation [13]−[17], human motion capture [18], computer graphics and games [19]−[21], molecular dynamics [22], and flight simulation [23]−[26]. Quaternions have no inherent geometrical singularity as Euler angles when parameterizing the 3-dimensional special orthogonal group manifold $\mathrm{SO}(3,\mathbb{R})$ with local coordinates and they are useful for real-time computation since only simple multiplications and additions are needed instead of trigonometric relations. Almost all of the researches available about the applications of quaternions focus on these two merits and the fundamental quaternion kinematical differential equation (QKDE) [1], [3], [8]. In [1], Robinson presented the following QKDE

$$\begin{cases} \dfrac{d\mathbb{q}}{dt} = \dfrac{1}{2}\boldsymbol{A}(\boldsymbol{\omega}(t)) \cdot \mathbb{q}, \quad t > t_0 \\ \mathbb{q}(t_0) = \mathbb{q}_0 \end{cases} \tag{1}$$

where t_0 is the initial time, $\boldsymbol{\omega} = [\omega_1(t), \omega_2(t), \omega_3(t)]^T$ is the angular velocity vector, $\mathbb{q} = [e_0, e_1, e_2, e_3]^T$ is the matrix representation of the quaternion $\mathbb{q}$ with scalar part e_0 as well as vector part $[e_1, e_2, e_3]^T$, and

$$\boldsymbol{A} = \boldsymbol{A}(\boldsymbol{\omega}(t)) = \begin{bmatrix} 0 & -\boldsymbol{\omega}^T \\ \boldsymbol{\omega} & -[\boldsymbol{\omega}]_\times \end{bmatrix} = -\boldsymbol{A}^T$$

$$[\boldsymbol{\omega}]_\times = \begin{bmatrix} 0 & -\omega_3 & \omega_2 \\ \omega_3 & 0 & -\omega_1 \\ -\omega_2 & \omega_1 & 0 \end{bmatrix} = -([\boldsymbol{\omega}]_\times)^T. \tag{2}$$

Formally, (1) is a linear ordinary differential equation (ODE) and its numerical solution should be easily determined in practical engineering applications. However, as Wie and Barbar [3] pointed out, the coefficients $\omega_1, \omega_2, \omega_3$, or equivalently the angular rate vector $\boldsymbol{\omega} = [\omega_1, \omega_2, \omega_3]^T$, are time-varying and the matrix $\boldsymbol{A}$ has the repeated eigenvalues

$$\pm j\|\boldsymbol{\omega}\| = \pm j\sqrt{\omega_1^2 + \omega_2^2 + \omega_3^2}$$

where $\|\cdot\|$ denotes the ℓ^2-norm. This implies that the linear time-varying system, i.e., the QKDE described by (1), is critically (neutrally) stable and the numerical integration is sensitive to the computational errors. Therefore, it is necessary to find a robust and long time precise integration method for solving (1). Many researchers have studied this problem with the traditional finite difference method since 1970s. Hrastar [27], Cunningham *et al.* [28] and Wie and Barbar [3] used the Taylor series method. Miller [29] tried the rotation vector concept. Mayo [30] adopted the Runge-Kutta [31] and the state transition matrix method. Wang and Zhang [32] compared the Runge-Kutta scheme with symplectic difference scheme, and Funda *et al.* [14] used the periodic normalization to unit magnitude. However, even for the time-invariant $\boldsymbol{\omega}$, the traditional numerical schemes for QKDE are sensitive to the

Manuscript received March 20, 2017; accepted September 29, 2017. This work was supported by the Fundamental Research Funds for the Central Universities of China (ZXH2012H005), and also supported in part by the National Natural Science Foundation of China (61201085, 51402356, 51506216), the Joint Fund of National Natural Science Foundation of China and Civil Aviation Administration of China (U1633101), and the Joint Fund of the Natural Science Foundation of Tianjin (15JCQNJC42800). Recommended by Associate Editor Maolin Ni. *(Corresponding author: Hong-Yan Zhang.)*

Citation: H.-Y. Zhang, Z.-H. Wang, L.-S. Zhou, Q.-N. Xue, L. Ma, and Y.-F. Niu, "Explicit symplectic geometric algorithms for quaternion kinematical differential equation," *IEEE/CAA J. of Autom. Sinica*, vol. 5, no. 2, pp. 479−488, Mar. 2018.

H.-Y. Zhang is with the School of Information Science and Technology, Hainan Normal University, Haikou 571158, China, and also with the Department of Engineering, Sino-European Institute of Aviation Engineering, Civil Aviation University of China, Tianjin 300300, China (e-mail: abs.hongyan@foxmail.com).

Z.-H. Wang, L.-S. Zhou, Q.-N. Xue, L. Ma, and Y.-F. Niu are with Civil Aviation University of China, Tianjin 300300, China (e-mail: zhwang0721@gmail.com; zlskulvzhe@163.com; qiannanxue@163.com; malong9904@aliyun.com; yifan45@foxmail.com).

Color versions of one or more of the figures in this paper are available online at http://ieeexplore.ieee.org.

Digital Object Identifier 10.1109/JAS.2017.7510829

accumulative computational errors in the sense of long time term.

In the past 30 years, the symplectic geometric algorithms (SGA) were originally proposed by Feng [33] and Ruth [34] independently and developed systematically by other researchers [35]−[39]. The advantage of SGA is that it can be used to solve the Hamiltonian system efficiently with a non-dissipative numerical scheme which avoids accumulative computational errors. For the ODE of time-varying system, the Gauss-Legendre (G-L) difference scheme [40], [41], an accurate and implicit Runge-Kutta method, is an implicit symplectic geometric algorithm (ISGA) essentially. However, it needs an extra iterative process to solve the numerical solution (NS). Its computational complexity is $O(n^2)$ [42] and thus, it is not appropriate for real-time applications.

We solve (1) via explicit symplectic geometric algorithms (ESGA) which overcomes the disadvantages of traditional non-symplectic difference schemes and symplectic G-L method. Firstly, we consider the autonomous QKDE (A-QKDE) with constant parameters ω_1, ω_2 and ω_3. The A-QKDE can be modelled with autonomous Hamiltonian system and solved by the SGA. Secondly, we discuss the non-autonomous QKDE (NA-QKDE) where $\omega_1(t), \omega_2(t), \omega_3(t)$ depend on time explicitly and design efficient difference scheme with symplectic method.

The main purpose of this paper is to propose ESGAs for solving the general NA-QKDE while preserving long time precision and the norms of quaternions automatically with linear time computation complexity. The contents of this paper are organized logically. The preliminaries of ESGA are presented in Section II. Section III deals with the ESGA for the A-QKDE. In Section IV we cope with the ESGA for NA-QKDE. The simulation results are presented in Section V. Finally, Section VI gives the summary and conclusions.

II. Preliminaries

A. Hamiltonian System

W. R. Hamilton introduced the canonical differential equations [43], [44]

$$\frac{dp_i}{dt} = -\frac{\partial H}{\partial q_i}, \quad \frac{dq_i}{dt} = \frac{\partial H}{\partial p_i}, \quad i = 1, 2, \dots, N$$

for problems of geometrical optics, where p_i are the generalized momentums, q_i are the generalized displacements and $H = H(p_1, \dots, p_N, q_1, \dots, q_N)$ is the Hamiltonian, viz., the total energy of the system. Let $\boldsymbol{p} = [p_1, \dots, p_N]^T \in \mathbb{R}^{N\times 1}$, $\boldsymbol{q} = [q_1, \dots, q_N]^T \in \mathbb{R}^{N\times 1}$, and $\boldsymbol{z} = [p_1, \dots, p_N, q_1, \dots, q_N]^T = [\boldsymbol{p}^T, \boldsymbol{q}^T]^T \in \mathbb{R}^{2N\times 1}$, then $H = H(\boldsymbol{p}, \boldsymbol{q}) = H(\boldsymbol{z})$ can be specified by $\boldsymbol{z}$ in the $2N$-dimensional phase space. Since the gradient of H is

$$H_{\boldsymbol{z}} = \left[\frac{\partial H}{\partial p_1}, \dots, \frac{\partial H}{\partial p_N}, \frac{\partial H}{\partial q_1}, \dots, \frac{\partial H}{\partial q_N}\right]^T \in \mathbb{R}^{2N\times 1}.$$

Then, the canonical equation is equivalent to

$$\frac{d\boldsymbol{z}}{dt} = \boldsymbol{J}_{2N}{}^{-1} \cdot H_{\boldsymbol{z}}(\boldsymbol{z}), \quad \boldsymbol{J}_{2N} = \begin{bmatrix} \boldsymbol{O}_N & \boldsymbol{I}_N \\ -\boldsymbol{I}_N & \boldsymbol{O}_N \end{bmatrix} \tag{3}$$

where $\boldsymbol{I}_N$ is the $N\times N$ identical matrix, $\boldsymbol{O}_N$ is the $N\times N$ zero matrix and $\boldsymbol{J}_{2N}$ is the $2N$th order standard symplectic matrix [33], [37]. For simplicity, the subscripts in $\boldsymbol{I}_N, \boldsymbol{I}_{2N}$ and $\boldsymbol{J}_{2N}$ may be omitted. Any system which can be described by (3) is called a Hamiltonian system. There are some fundamental properties for the canonical equation of Hamiltonian system [43], [45]−[47]:

1) it is invariant under the symplectic transform (phase flow);

2) the evolution of the system is the evolution of symplectic transform;

3) the symplectic symmetry and the total energy of the system can be preserved simultaneously and automatically.

B. Transition Matrix

The SGA was motivated by the three fundamental properties 1)−3). Ruth [34] and Feng [33] emphasized two key points in their pioneering works:

a) SGA is a kind of difference scheme which preserves the symplectic structure of Hamiltonian system;

b) the single-step transition matrix is a symplectic transform (matrix) which preserves the symplectic structure of the difference equation (discrete version) of the continuous form of (3).

Let τ be the time step and $\boldsymbol{z}[k] = \boldsymbol{z}(t_0 + k\tau)$ be the sample value at the discrete time $t_k = t_0 + k\tau$. With the initial condition

$$\boldsymbol{z}[0] = [p_1(t_0), \dots, p_N(t_0), q_1(t_0), \dots, q_N(t_0)]^T \tag{4}$$

the symplectic difference scheme (SDS) for (3) is given by

$$\boldsymbol{z}[k+1] = \boldsymbol{g}_\tau \boldsymbol{z}[k], \quad k = 0, 1, 2, \dots$$
$$\boldsymbol{G}_\tau = \frac{\partial \boldsymbol{z}[k+1]}{\partial \boldsymbol{z}[k]} = \frac{\partial(\boldsymbol{g}_\tau \boldsymbol{z}[k])}{\partial \boldsymbol{z}[k]} \in \mathbb{R}^{2N\times 2N} \tag{5}$$

where $\boldsymbol{g}_\tau : \mathbb{R}^{2N\times 1} \to \mathbb{R}^{2N\times 1}$ is the transition operator, also named the transition mapping, and $\boldsymbol{G}_\tau$ is the transition matrix (Jacobi matrix) of $\boldsymbol{g}_\tau$ at $\boldsymbol{z}[k]$ such that $\boldsymbol{G}_\tau$ is symplectic, viz.,

$$\boldsymbol{G}_\tau^T \boldsymbol{J} \boldsymbol{G}_\tau = \boldsymbol{J}. \tag{6}$$

Equivalently, we have $\boldsymbol{G}_\tau \in \mathrm{Sp}(2N, \mathbb{R}) \subset \mathrm{GL}(2N, \mathbb{R}) \subset \mathbb{R}^{2N\times 2N}$, in which $\mathrm{Sp}(2N, \mathbb{R})$ is the symplectic transform group and $\mathrm{GL}(2N, \mathbb{R})$ is the general linear transform group [48]−[50]. When designing SGA, the key problem is to determine the $\boldsymbol{g}_\tau$ or its Jacobi matrix $\boldsymbol{G}_\tau$ since both of them can be used to construct the SDS of interest. In this paper, we will find the symplectic matrix $\boldsymbol{G}_\tau$ and we always have $\boldsymbol{g}_\tau = \boldsymbol{G}_\tau$ since (1) is a linear ODE.

For the general non-linear and non-separable Hamiltonian system, the centered Euler implicit scheme (CEIS) is a widely used SGA with second order precision. It is described by [37]

$$\frac{\boldsymbol{p}[k+1] - \boldsymbol{p}[k]}{\tau} = -H_{\boldsymbol{q}}(\bar{\boldsymbol{z}}_k)$$
$$\frac{\boldsymbol{q}[k+1] - \boldsymbol{q}[k]}{\tau} = H_{\boldsymbol{p}}(\bar{\boldsymbol{z}}_k) \tag{7}$$

in which the midpoint $\bar{\boldsymbol{z}}_k$ is defined by

$$\bar{\boldsymbol{z}}_k = \frac{\boldsymbol{z}[k+1] + \boldsymbol{z}[k]}{2}. \tag{8}$$

The CEIS can be used to find the transition matrix $\boldsymbol{G}_\tau$. Let

$$\boldsymbol{B} = \boldsymbol{J}^{-1} H_{\boldsymbol{zz}}(\bar{\boldsymbol{z}}_k) \tag{9}$$

where $H_{\boldsymbol{zz}}(\cdot) = (\frac{\partial^2 H(\cdot)}{\partial z_i \partial z_j})_{2N\times 2N}$ is the Hessel matrix at the midpoint $\bar{\boldsymbol{z}}_k$, and

$$\phi(\lambda) = \frac{1+\lambda}{1-\lambda} = (1+\lambda)(1-\lambda)^{-1} \tag{10}$$

be the Cayley transform. Then, for small τ such that $\boldsymbol{I} - \frac{\tau}{2}\boldsymbol{B}$ is non-singular, we have [37]

$$\boldsymbol{G}_\tau = \phi\left(\frac{\tau}{2}\boldsymbol{B}\right) = \left[\boldsymbol{I} + \frac{\tau}{2}\boldsymbol{B}\right] \cdot \left[\boldsymbol{I} - \frac{\tau}{2}\boldsymbol{B}\right]^{-1}. \tag{11}$$

Note that although (11) is an approximate result in the sense of approximate conservation [33] for the general non-linear Hamiltonian system (linear Hamiltonian system requires that the Hessel matrix $H_{\boldsymbol{zz}}(\cdot)$ is symmetric), it could be a precise solution for some special cases.

III. Symplectic Algorithm for A-QKDE

A. A-QKDE and Autonomous Hamiltonian System

When the matrix $\boldsymbol{A}$ in (1) is time-invariant, or equivalently the parameters ω_1, ω_2 and ω_3 are constants, we can model (1) with the autonomous Hamiltonian system. Putting $N = 2$, $\boldsymbol{p} = [p_1, p_2]^T = [e_0, e_1]^T$, $\boldsymbol{q} = [q_1, q_2]^T = [e_2, e_3]^T$, $\mathbb{q} = [\boldsymbol{p}^T, \boldsymbol{q}^T]^T \equiv \boldsymbol{z}$, we can obtain

$$\frac{d\boldsymbol{z}}{dt} = \boldsymbol{J}^{-1} H_{\boldsymbol{z}}(\boldsymbol{z}) = \frac{1}{2}\boldsymbol{A}(\boldsymbol{\omega})\boldsymbol{z} \tag{12}$$

by (1) and (2). We remark here that the notation $\boldsymbol{z}$ is usually used in the literatures about SGA while notation $\mathbb{q}$ is used in references about quaternions. The equivalence shows that $\mathbb{q}$ and $\boldsymbol{z}$ can be used alternatively if necessary. From (12) we can find that $\boldsymbol{J}^{-1}H_{\boldsymbol{z}}(\boldsymbol{z}) = \frac{1}{2}\boldsymbol{A}\boldsymbol{z}$. Therefore

$$\begin{aligned}\boldsymbol{A} &= 2\boldsymbol{J}^{-1}H_{\boldsymbol{zz}}(\boldsymbol{z})\\ H_{\boldsymbol{zz}}(\boldsymbol{z}) &= \frac{1}{2}\boldsymbol{J}\boldsymbol{A}\\ \boldsymbol{B} &= \boldsymbol{J}^{-1}H_{\boldsymbol{zz}}(\boldsymbol{z}) = \frac{1}{2}\boldsymbol{A}\end{aligned} \tag{13}$$

according to (9). Note that $\boldsymbol{JA} \neq \boldsymbol{AJ}$, so the Hessel matrix $H_{\boldsymbol{zz}}(\boldsymbol{z})$ is not symmetric, which means that the Hamiltonian system here is nonlinear by definition [37]. Obviously, the A-QKDE is an autonomous Hamiltonian system and the SGA can be adopted.

B. Symplectic Transition Matrix

We now prove some interesting lemmas and theorems for constructing the SDS for A-QKDE.

Lemma 1 (Generalized Euler's formula): Suppose matrix $\boldsymbol{M} \in \mathbb{R}^{n\times n}$ is skew-symmetric, i.e., $\boldsymbol{M}^T = -\boldsymbol{M}$, and there exists a positive constant γ such that $\boldsymbol{M}^2 = -\gamma^2\boldsymbol{I}$. Let $\hat{\boldsymbol{M}} = \gamma^{-1}\boldsymbol{M}$, then $\hat{\boldsymbol{M}}^2 = -\boldsymbol{I}$. For any $x \in \mathbb{R}$, we have

$$\exp(x\boldsymbol{M}) = \cos(x\gamma)\boldsymbol{I} + \sin(x\gamma)\hat{\boldsymbol{M}}. \tag{14}$$

Proof:

$$\begin{aligned}\exp(x\boldsymbol{M}) &= \sum_{k=0}^{\infty} \frac{(x\boldsymbol{M})^k}{k!}\\ &= \sum_{k=0}^{\infty} \frac{(x\boldsymbol{M})^{2k}}{(2k)!} + \sum_{k=0}^{\infty} \frac{(x\boldsymbol{M})^{2k+1}}{(2k+1)!}\\ &= \sum_{k=0}^{\infty}(-\gamma^2)^k\boldsymbol{I}\frac{x^{2k}}{(2k)!} + \sum_{k=0}^{\infty}(-\gamma^2)^k\boldsymbol{M}\frac{x^{2k+1}}{(2k+1)!}\\ &= \boldsymbol{I}\sum_{k=0}^{\infty}(-1)^k\frac{(x\gamma)^{2k}}{(2k)!} + \frac{\boldsymbol{M}}{\gamma}\sum_{k=0}^{\infty}(-1)^k\frac{(x\gamma)^{2k+1}}{(2k+1)!}\\ &= \cos(x\gamma)\boldsymbol{I} + \hat{\boldsymbol{M}}\sin(x\gamma).\end{aligned}$$

■

Lemma 2 (Cayley-Euler formula): Suppose matrix $\boldsymbol{M} \in \mathbb{R}^{n\times n}$ is skew-symmetric, i.e., $\boldsymbol{M}^T = -\boldsymbol{M}$, and there exists a positive constant γ such that $\boldsymbol{M}^2 = -\gamma^2\boldsymbol{I}$. Let $\hat{\boldsymbol{M}} = \gamma^{-1}\boldsymbol{M}$, then $\hat{\boldsymbol{M}}^2 = -\boldsymbol{I}$. Let $\phi(\lambda)$ be the Cayley transformation, then for any $x \in \mathbb{R}$ the Cayley-Euler formula

$$\begin{aligned}\phi(x\boldsymbol{M}) &= \frac{\boldsymbol{I} + x\boldsymbol{M}}{\boldsymbol{I} - x\boldsymbol{M}}\\ &= \frac{1}{1+\alpha}[(1-\alpha)\boldsymbol{I} + 2x\boldsymbol{M}]\\ &= \cos\theta(x,\gamma)\boldsymbol{I} + \sin\theta(x,\gamma)\hat{\boldsymbol{M}}\\ &= \exp(\theta(x,\gamma)\boldsymbol{M})\end{aligned} \tag{15}$$

holds, in which $\theta = \theta(x,\gamma) = 2\cdot\arctan(x\gamma)$ and $\alpha = x^2\gamma^2$. Furthermore, $\phi(x\boldsymbol{M})$ is an orthogonal matrix.

Proof: It is trivial that $\hat{\boldsymbol{M}}^T = -\hat{\boldsymbol{M}}$ and $\hat{\boldsymbol{M}}^2 = -\boldsymbol{I}$. For any $x \in \mathbb{R}$, we find that $(\boldsymbol{I} - x\boldsymbol{M})(\boldsymbol{I} + x\boldsymbol{M}) = (1 + x^2\gamma^2)\boldsymbol{I}$. In consequence $(\boldsymbol{I} - x\boldsymbol{M})^{-1} = \frac{1}{1+x^2\gamma^2}(\boldsymbol{I} + x\boldsymbol{M})$. Hence the Cayley transformation $\phi(x\boldsymbol{M})$ can be simplified as following

$$\begin{aligned}\phi(x\boldsymbol{M}) &= (\boldsymbol{I} - x\boldsymbol{M})^{-1}(\boldsymbol{I} + x\boldsymbol{M})\\ &= \frac{1}{1+\alpha}[(1-\alpha)\boldsymbol{I} + 2x\boldsymbol{M}]\end{aligned} \tag{16}$$

where $\alpha = x^2\gamma^2$. Let $\tan(\theta/2) = x\gamma$, then by the trigonometric identity, $\boldsymbol{M} = \gamma\hat{\boldsymbol{M}}$ and Lemma 1, we immediately have

$$\begin{aligned}\phi(x\boldsymbol{M}) &= \frac{1}{1+x^2\gamma^2}[(1 - x^2\gamma^2)\boldsymbol{I} + 2x\gamma\hat{\boldsymbol{M}}]\\ &= \cos\theta(x,\gamma)\boldsymbol{I} + \sin\theta(x,\gamma)\hat{\boldsymbol{M}}\\ &= \exp(\theta(x,\gamma)\boldsymbol{M}).\end{aligned} \tag{17}$$

Moreover,

$$\begin{aligned}&[\phi(x\boldsymbol{M})]^T \cdot \phi(x\boldsymbol{M})\\ &\quad= [\cos\theta(x,\gamma)\boldsymbol{I} + \sin\theta(x,\gamma)\hat{\boldsymbol{M}}]^T\\ &\qquad\cdot [\cos\theta(x,\gamma)\boldsymbol{I} + \sin\theta(x,\gamma)\hat{\boldsymbol{M}}]\\ &\quad= \cos^2\theta(x,\gamma)\boldsymbol{I} - \sin^2\theta(x,\gamma)\hat{\boldsymbol{M}}^2 = \boldsymbol{I}.\end{aligned}$$

Similarly, we can obtain $\phi(x\boldsymbol{M}) \cdot [\phi(x\boldsymbol{M})]^T = \boldsymbol{I}$. Hence $\phi(x\boldsymbol{M})$ is orthogonal by definition. ■

Theorem 1: For any time step τ and time-invariant vector $\boldsymbol{\omega}$, the transition matrix $\boldsymbol{G}_\tau^{\mathbb{q}}$ for the A-QKDE is

$$\begin{aligned}\boldsymbol{G}_\tau^{\mathrm{q}} &= \frac{1}{1+\alpha}\left[(1-\alpha)\boldsymbol{I} + \frac{\tau}{2}\boldsymbol{A}\right] \\ &= \cos\theta(\boldsymbol{\omega},\tau)\cdot\boldsymbol{I} + \sin\theta(\boldsymbol{\omega},\tau)\cdot\hat{\boldsymbol{A}} \\ &= \exp(\theta(\boldsymbol{\omega},\tau)\boldsymbol{A}) \end{aligned} \tag{18}$$

in which $\alpha = \tau^2\|\boldsymbol{\omega}\|^2/16$, $\theta = 2\arctan(\tau\|\boldsymbol{\omega}\|/4)$, $\hat{\boldsymbol{A}} = \boldsymbol{A}/\|\boldsymbol{\omega}\|$ and $\hat{\boldsymbol{A}}^2 = -\boldsymbol{I}$.

Proof: With the help of (11) and (13), the transition matrix will be $\boldsymbol{G}_\tau^{\mathrm{q}} = \phi\left(\frac{\tau}{2}\boldsymbol{B}_{\boldsymbol{z}}\right) = \phi\left(\frac{\tau}{4}\boldsymbol{A}\right)$. Let $x = \tau/4$, $\boldsymbol{M} = \boldsymbol{A}$, $\gamma = \|\boldsymbol{\omega}\|$, then $\alpha = x^2\gamma^2 = \|\boldsymbol{\omega}\|^2\tau^2/16$. Thus the theorem follows from Lemma 2 directly. ■

Theorem 2: For any $\boldsymbol{\omega} \in \mathbb{R}^{3\times 1}$ and $\tau \in \mathbb{R}$, the transition matrix $\boldsymbol{G}_\tau^{\mathrm{q}}$ is an orthogonal transformation and an invertible symplectic transformation with second order precision, i.e.,

$$[\boldsymbol{G}_\tau^{\mathrm{q}}]^T\boldsymbol{J}\boldsymbol{G}_\tau^{\mathrm{q}} = \boldsymbol{J}, \quad [\boldsymbol{G}_\tau^{\mathrm{q}}]^{-1} = \boldsymbol{G}_{-\tau}^{\mathrm{q}} = [\boldsymbol{G}_\tau^{\mathrm{q}}]^T. \tag{19}$$

Proof: For a constant vector $\boldsymbol{\omega}$, we can find the function $\theta = 2\arctan(\tau\|\boldsymbol{\omega}\|/4)$ is an odd function of time step τ. By utilizing $\hat{\boldsymbol{A}}^2 = -\boldsymbol{I}$ and $\hat{\boldsymbol{A}}^T = -\hat{\boldsymbol{A}}$, we immediately obtain

$$\begin{aligned}[\boldsymbol{G}_\tau^{\mathrm{q}}]^T &= [\cos\theta(\boldsymbol{\omega},\tau)\boldsymbol{I} + \sin\theta(\boldsymbol{\omega},\tau)\hat{\boldsymbol{A}}]^T \\ &= \cos\theta(\boldsymbol{\omega},\tau)\boldsymbol{I} - \sin\theta(\boldsymbol{\omega},\tau)\hat{\boldsymbol{A}} \\ &= \cos(-\theta(\boldsymbol{\omega},\tau))\boldsymbol{I} + \sin(-\theta(\boldsymbol{\omega},\tau))\hat{\boldsymbol{A}} \\ &= \cos\theta(\boldsymbol{\omega},-\tau))\boldsymbol{I} + \sin\theta(\boldsymbol{\omega},-\tau)\hat{\boldsymbol{A}} \\ &= \boldsymbol{G}_{-\tau}^{\mathrm{q}}\end{aligned}$$

which implies that the transition matrix is invertible. Moreover, $\boldsymbol{G}_\tau^{\mathrm{q}}$ is orthogonal by Lemma 2. In consequence, $[\boldsymbol{G}_\tau^{\mathrm{q}}]^T = \boldsymbol{G}_{-\tau}^{\mathrm{q}} = (\boldsymbol{G}_\tau^{\mathrm{q}})^{-1}$. Furthermore, simple algebraic operation implies that

$$\boldsymbol{J}\hat{\boldsymbol{A}} - \hat{\boldsymbol{A}}\boldsymbol{J} = \frac{1}{\|\boldsymbol{\omega}\|}(\boldsymbol{J}\boldsymbol{A} - \boldsymbol{A}\boldsymbol{J}) = \boldsymbol{O}$$

$$\hat{\boldsymbol{A}}\boldsymbol{J}\hat{\boldsymbol{A}} = \frac{1}{\|\boldsymbol{\omega}^2\|}\boldsymbol{A}\boldsymbol{J}\boldsymbol{A} = -\boldsymbol{J}$$

and $\hat{\boldsymbol{A}}^{-1} = -\hat{\boldsymbol{A}}$. Therefore,

$$\begin{aligned}[\boldsymbol{G}_\tau^{\mathrm{q}}]^T\boldsymbol{J}[\boldsymbol{G}_\tau^{\mathrm{q}}] &= (\cos\theta\boldsymbol{I} + \sin\theta\hat{\boldsymbol{A}})^T\boldsymbol{J}(\cos\theta\boldsymbol{I} + \sin\theta\hat{\boldsymbol{A}}) \\ &= (\cos\theta\boldsymbol{I} - \sin\theta\hat{\boldsymbol{A}})\boldsymbol{J}(\cos\theta\boldsymbol{I} + \sin\theta\hat{\boldsymbol{A}}) \\ &= \cos^2\theta\boldsymbol{J} - \sin^2\theta\hat{\boldsymbol{A}}\boldsymbol{J}\hat{\boldsymbol{A}} + \cos\theta\sin\theta(\boldsymbol{J}\hat{\boldsymbol{A}} - \hat{\boldsymbol{A}}\boldsymbol{J}) \\ &= \boldsymbol{J}.\end{aligned}$$

Hence $\boldsymbol{G}_\tau^{\mathrm{q}}$ is a symplectic matrix. Since the $\boldsymbol{G}_\tau^{\mathrm{q}}$ is constructed from CEIS directly, it must be a second order precision scheme. ■

C. Comparison With Analytic Solution

Fortunately, the analytic solution (AS) for A-QKDE can be found without difficulty. In fact for any $t \in [t_0, t_f]$ where t_0 and t_f denote the initial and final time respectively, we have

$$\mathrm{q}(t) = \exp\left(\frac{1}{2}\boldsymbol{A}\cdot(t-t_0)\right)\cdot\mathrm{q}(t_0), \quad t\in[t_0,t_f]. \tag{20}$$

Let $x = (t-t_0)/2$ and $\hat{\boldsymbol{A}} = \boldsymbol{A}/\|\boldsymbol{\omega}\|$, then $\boldsymbol{A}^2 = -\|\boldsymbol{\omega}\|^2\boldsymbol{I}$ implies that

$$\exp(\boldsymbol{A}x) = \cos\left(\frac{\|\boldsymbol{\omega}\|(t-t_0)}{2}\right)\boldsymbol{I} + \sin\left(\frac{\|\boldsymbol{\omega}\|(t-t_0)}{2}\right)\hat{\boldsymbol{A}}$$

by Lemma 1. Thus for $t - t_0 = \tau$, the AS to the transition matrix for the A-QKDE is

$$\boldsymbol{G}_{\tau,\mathrm{AS}}^{\mathrm{q}} = \boldsymbol{I}\cos\frac{\|\boldsymbol{\omega}\|\tau}{2} + \hat{\boldsymbol{A}}\sin\frac{\|\boldsymbol{\omega}\|\tau}{2} \quad \forall\tau\in\mathbb{R}. \tag{21}$$

At the same time, for sufficiently small τ in (18) we have

$$\begin{aligned}\boldsymbol{G}_\tau^{\mathrm{q}} &= \boldsymbol{I}\cos\left(2\arctan\frac{\|\boldsymbol{\omega}\|\tau}{4}\right) + \hat{\boldsymbol{A}}\sin\left(2\arctan\frac{\|\boldsymbol{\omega}\|\tau}{4}\right) \\ &\sim \boldsymbol{I}\cos\frac{\|\boldsymbol{\omega}\|\tau}{2} + \hat{\boldsymbol{A}}\sin\frac{\|\boldsymbol{\omega}\|\tau}{2}\end{aligned} \tag{22}$$

for sufficiently small $x = \|\boldsymbol{\omega}\tau\|$ since

$$\begin{aligned}f_1(x) &= \cos\frac{x}{2} - \cos\left(2\arctan\frac{x}{4}\right) \\ &= -\frac{x^4}{192} + \frac{43x^6}{92\,160} - \frac{157x^8}{5\,160\,960} \\ &\quad + \frac{14\,173x^{10}}{7431\,782\,400} + O(x^{12}) \\ f_2(x) &= \sin\frac{x}{2} - \sin\left(2\arctan\frac{x}{4}\right) \\ &= \frac{x^3}{96} - \frac{13x^5}{7680} + \frac{311x^7}{2\,580\,480} - \frac{2833x^9}{371\,589\,120} + O(x^{11}).\end{aligned}$$

Let $r = \max_{x\in\mathbb{R}^+}\{|f_1(x)|, |f_2(x)|\}$, then we have $r < 1.25 \times 10^{-4}$ for $x \le 0.2$ and $r < 1.57\times 10^{-8}$ for $x \le 0.01$. Therefore, the $\boldsymbol{G}_{\tau,AS}^{\mathrm{q}}$ can be approximated by $\boldsymbol{G}_\tau^{\mathrm{q}}$ with an acceptable precision when time step $\tau \le 1/(5\|\boldsymbol{\omega}\|)$.

D. Explicit Symplectic Geometric Algorithm for A-QKDE

The ESGA for A-QKDE based on CEIS, ESGA-I for brevity, is given in Algorithm 1 by the explicit expression of $\boldsymbol{G}_\tau^{\mathrm{q}}$ obtained.

Algorithm 1 Explicit Symplectic Geometric Algorithm for A-QKDE (ESGA-I)

Require: The time-invariant vector $\boldsymbol{\omega} \in \mathbb{R}^{3\times 1}$, time step τ and the initial quaternion q_0 at initial time t_0.

Ensure: Numerical solution to the A-QKDE $\frac{d\mathrm{q}}{dt} = \frac{1}{2}\boldsymbol{A}(\boldsymbol{\omega})\mathrm{q}$ for $t \ge t_0$ with second order SDS.

1: Set matrix $\boldsymbol{A}$ with vector $\boldsymbol{\omega} = [\omega_1, \omega_2, \omega_3]^T$ via (2).
2: Set parameter α with $\boldsymbol{\omega}$ and τ, viz. $\alpha = \frac{1}{16}\tau^2\|\boldsymbol{\omega}\|^2 = \frac{1}{16}\tau^2(\omega_1^2 + \omega_2^2 + \omega_3^2)$.
3: Compute the transition matrix: $\boldsymbol{G}_\tau^{\mathrm{q}} = \frac{1}{1+\alpha}\left[(1-\alpha)\boldsymbol{I} + \frac{\tau}{2}\boldsymbol{A}\right]$.
4: Set the initial condition $\mathrm{q}[0] = \mathrm{q}(t_0) = \mathrm{q}_0$.
5: Iterate: $\mathrm{q}[k+1] = \boldsymbol{G}_\tau^{\mathrm{q}}\mathrm{q}[k]$, $k = 0, 1, 2, \ldots$.

Suppose that the time consumed for the multiplication and addition of real numbers are δ_1 and δ_2, respectively, the function invoking time is ignored and there are n iterations in Step 5. Table I shows that the total time consumed (without optimization) is $20(2\delta_1 + \delta_2) + (16\delta_1 + 12\delta_2)n = O(n)$. Therefore, the time complexity is linear. Moreover, we have to store $\omega_1, \omega_2, \omega_3, \boldsymbol{A}, \tau, \alpha, \boldsymbol{G}_\tau^{\mathrm{q}}, k$ and $\mathrm{q}[k]$. Note that all of the $\mathrm{q}[k]$ share a common storage and only 43 real numbers should be stored in this algorithm. Obviously, the space complexity is constant, i.e., $O(1)$.

TABLE I
TIME AND SPACE CONSUMPTIONS OF ESGA-I

Step	Time for $*$	Time for $+$	Real numbers to be stored
0	-	-	$t_0, \tau, \omega_1, \omega_2, \omega_3$
1	-	-	$\boldsymbol{A} \in \mathbb{R}^{4\times 4}$
2	$6\delta_1$	$2\delta_2$	α
3	$34\delta_1$	$18\delta_2$	$\boldsymbol{G}_\tau^{\mathrm{q}} \in \mathbb{R}^{4\times 4}$
4	-	-	$\mathrm{q}[0] \in \mathbb{R}^{4\times 1}$
5	$16n\delta_1$	$12n\delta_2$	$k, \mathrm{q}[k]$

IV. SYMPLECTIC GEOMETRIC METHOD FOR NA-QKDE

A. Time-dependent Parameters and NA-QKDE

For the time-varying vector $\boldsymbol{\omega} = \boldsymbol{\omega}(t)$, (1) implies $\dot{\boldsymbol{z}} = \boldsymbol{J}^{-1} H_{\boldsymbol{z}}(\boldsymbol{z}) = \frac{1}{2}\boldsymbol{A}(\boldsymbol{\omega}(t))\boldsymbol{z}$, where $H = H(p_1, p_2, q_1, q_2, t) = H(e_0, e_1, e_2, e_3, t)$. Hence the NA-QKDE is a non-autonomous Hamiltonian system essentially and the corresponding SGA can be obtained via the concept of extended phase space [37]. Let $p_3 = h, q_3 = t$, where h is the negative of the total energy. Let $\boldsymbol{z} = [p_1, p_2, h, q_1, q_2, t]^T = [\boldsymbol{p}^T, h, \boldsymbol{q}^T, t]^T \in \mathbb{R}^{(2N+2)\times 1}$, $K(\tilde{\boldsymbol{z}}) = h + H(p_1, p_2, q_1, q_2, t) = h + H(\boldsymbol{p}, \boldsymbol{q}, t) = h + H(\mathrm{q}, t)$, then we have the time-centered Euler implicit scheme (T-CEIS) with fourth order [37],

$$\frac{\boldsymbol{z}[k+1] - \boldsymbol{z}[k]}{\tau} = \boldsymbol{J}^{-1} H_{\boldsymbol{z}}(\bar{\boldsymbol{z}}_k) - \frac{\tau^2}{24}\boldsymbol{J}^{-1} \cdot \nabla_{\boldsymbol{z}}\left\{[H_{\boldsymbol{z}}(\bar{\boldsymbol{z}}_k)]^T \boldsymbol{J}^{-1} H_{\boldsymbol{z}\boldsymbol{z}}(\bar{\boldsymbol{z}}_k)\boldsymbol{J}^{-1} H_{\boldsymbol{z}}(\bar{\boldsymbol{z}}_k)\right\}. \quad (23)$$

Equation (23) shows that for the time-varying problems, $H_*(\bar{\boldsymbol{z}}_k)$ is replaced by $H_*(\bar{\boldsymbol{z}}_k, \bar{t}_k)$ where $*$ may be $\boldsymbol{p}$, $\boldsymbol{q}$ or t. In order to guarantee the duality of the phase space, we take $\boldsymbol{z} = [\boldsymbol{p}^T, \boldsymbol{q}^T]^T$. The symplectic scheme for the NA-QKDE as (23) can be simplified as

$$\frac{\boldsymbol{z}[k+1] - \boldsymbol{z}[k]}{\tau} = \frac{1}{2}\boldsymbol{A}_k \bar{\boldsymbol{z}}_k - \frac{\tau^2 \Omega_k \|\boldsymbol{\omega}_k\|^2}{96}\boldsymbol{J}\bar{\boldsymbol{z}}_k \quad (24)$$

where $\bar{t}_k = t[k] + \tau/2$, $\boldsymbol{\omega}_k = \boldsymbol{\omega}(\bar{t}_k)$, $\boldsymbol{A}_k = \boldsymbol{A}(\boldsymbol{\omega}_k)$ and

$$\Omega_k = \omega_2(\bar{t}_k). \quad (25)$$

By taking the similar procedure as we do in finding the transition matrix for SDS of the A-QKDE, we can obtain

$$\boldsymbol{G}_\tau^{\mathrm{q}}(k+1|k) = \left[\boldsymbol{I} - \frac{\tau}{2}\boldsymbol{B}_k\right]^{-1}\left[\boldsymbol{I} + \frac{\tau}{2}\boldsymbol{B}_k\right] \quad (26)$$

where $\boldsymbol{B}_k$ is a skew-symmetric matrix such that

$$\boldsymbol{B}_k = \frac{1}{2}\boldsymbol{A}_k - \frac{\tau^2 \Omega_k \|\boldsymbol{\omega}_k\|^2}{96}\boldsymbol{J} = -\boldsymbol{B}_k^T. \quad (27)$$

According to Lemma 2, there exists a series of γ_k such that

$$\boldsymbol{B}_k^2 = -\gamma_k^2 \boldsymbol{I}. \quad (28)$$

Theorem 3: For the NA-QKDE $\frac{d\mathrm{q}}{dt} = \frac{1}{2}\boldsymbol{A}[\boldsymbol{\omega}(t)]\mathrm{q}$, let $\beta_k = -\frac{\tau^2}{96}\Omega_k\|\boldsymbol{\omega}_k\|^2$, $\gamma_k^2 = \frac{1}{4}\|\boldsymbol{\omega}_k\|^2 - \beta_k\Omega_k + \beta_k^2$, $\alpha_k = \frac{\tau^2}{4}\gamma_k^2 = \frac{1}{16}\tau^2\|\boldsymbol{\omega}_k\|^2(1 + \frac{\tau^2\Omega_k^2}{24} + \frac{\tau^4\Omega_k^2\|\boldsymbol{\omega}_k\|^2}{2304})$, $\hat{\boldsymbol{B}}_k = \frac{1}{\gamma_k}\boldsymbol{B}_k$, then for $k = 0, 1, 2, \ldots$, the transition matrix $\boldsymbol{G}_\tau^{\mathrm{q}}(k+1|k) : \boldsymbol{z}[k] \mapsto \boldsymbol{z}[k+1]$ will be

$$\begin{aligned}\boldsymbol{G}_\tau^{\mathrm{q}}(k+1|k) &= \frac{1}{1+\alpha_k}[(1-\alpha_k)\boldsymbol{I} + \tau\boldsymbol{B}_k] \\ &= \cos\theta(\boldsymbol{\omega}_k, \tau)\boldsymbol{I} + \sin\theta(\boldsymbol{\omega}_k, \tau)\hat{\boldsymbol{B}}(\boldsymbol{\omega}_k) \quad (29)\end{aligned}$$

such that

$$[\boldsymbol{G}_\tau^{\mathrm{q}}(k+1|k)]^T \cdot \boldsymbol{J} \cdot [\boldsymbol{G}_\tau^{\mathrm{q}}(k+1|k)] = \boldsymbol{J} \quad (30)$$

where $\theta = 2\arctan\left[\frac{\tau\|\boldsymbol{\omega}_k\|}{4}\sqrt{1 + \frac{\tau^2}{24}\Omega_k^2 + \frac{\tau^4}{2304}\Omega_k^2\|\boldsymbol{\omega}_k\|^2}\right]$.

We remark that this SDS is a fourth order scheme according to [37]. In addition, since $\boldsymbol{\omega}(t)$ is time-dependent and $\boldsymbol{\omega}(t[k] - \tau/2) \neq \boldsymbol{\omega}(t[k] + \tau/2)$ for positive τ in general, we can deduce that $\boldsymbol{G}_{-\tau}^{\mathrm{q}}(k+1|k) \neq [\boldsymbol{G}_\tau^{\mathrm{q}}(k+1|k)]^{-1}$ although $\boldsymbol{G}_\tau^{\mathrm{q}}(k+1|k)$ is also a symplectic and orthogonal transformation.

B. Explicit Symplectic Geometric Scheme for NA-QKDE

The ESGA for NA-QKDE based on T-CEIS, ESGA-II for brevity, is presented in Algorithm 2. With the similar complexity calculations for Algorithm 1, we can find that the time complexity and space complexity of Algorithm 2 are also $O(n)$ and $O(1)$, respectively.

Algorithm 2 Explicit Symplectic Geometric Algorithm for NA-QKDE (ESGA-II)

Require: The time-varying vector $\boldsymbol{\omega}(t) \in \mathbb{R}^{3\times 1}$, initial time t_0, initial quaternion q_0 and time step τ.

Ensure: Numerical solution to the NA-QKDE $\frac{d\mathrm{q}}{dt} = \frac{1}{2}\boldsymbol{A}(\boldsymbol{\omega}(t))\mathrm{q}$ for $t \geq t_0$ with fourth order SDS.

1: Set the initial condition $\mathrm{q}[0] = \mathrm{q}(t_0) = \mathrm{q}_0$.
2: set $\bar{t}_k = t_0 + (k + 1/2)\tau$.
3: Set matrix $\boldsymbol{A}_k$ with vector $\boldsymbol{\omega}_k = [\omega_1(\bar{t}_k), \omega_2(\bar{t}_k), \omega_3(\bar{t}_k)]^T$ according to (2) and $\Omega_k = \omega_2(\bar{t}_k)$ by (25).
4: Calculate the norm of $\boldsymbol{\omega}_k$:
$\|\boldsymbol{\omega}_k\|^2 = [\omega_1(\bar{t}_k)]^2 + [\omega_2(\bar{t}_k)]^2 + [\omega_3(\bar{t}_k)]^2$.
5: Set parameters β_k and α_k:
$\beta_k = -\frac{\tau^2}{96}\Omega_k\|\boldsymbol{\omega}_k\|^2$
$\alpha_k = \frac{1}{4}\tau^2(\frac{1}{4}\|\boldsymbol{\omega}_k\|^2 - \Omega_k\beta_k + \beta_k^2)$.
6: Set matrix $\boldsymbol{B}_k$ with $\boldsymbol{\omega}_k$ and τ according to (27).
7: Compute the transition matrix:
$\boldsymbol{G}_\tau^{\mathrm{q}}(k+1|k) = \frac{1}{1+\alpha_k}[(1-\alpha_k)\boldsymbol{I} + \tau\boldsymbol{B}_k]$.
8: Iterate: $\mathrm{q}[k+1] = \boldsymbol{G}_\tau^{\mathrm{q}}(k+1|k)\mathrm{q}[k], \quad k = 0, 1, 2, \ldots$.

We remark here that $\boldsymbol{\omega}_k = \boldsymbol{\omega}(\bar{t}_k) = \boldsymbol{\omega}(t[k] + \tau/2)$ relates the fractional interval sampling, which will increase the complexity of the hardware implementation. However, if the sampling rate $f_s = 1/\tau$ is large enough, the $\boldsymbol{\omega}(t)$ will vary slowly in each short time interval $[t[k], t[k+1]]$ and the linear interpolation can be considered here. This is to say that for $t \in [t[k], t[k+1]]$

$$\boldsymbol{\omega}(t) \approx \boldsymbol{\omega}(t[k]) + \frac{\boldsymbol{\omega}(t[k+1]) - \boldsymbol{\omega}(t[k])}{\tau}t. \quad (31)$$

Hence

$$\boldsymbol{\omega}(\bar{t}_k) \approx \boldsymbol{\omega}(t[k]) + \frac{\boldsymbol{\omega}(t[k+1]) - \boldsymbol{\omega}(t[k])}{\tau}\bar{t}_k \tag{32}$$

with acceptable precision. In this way the fractional interval sampling can be avoided and the complexity of the hardware implementation can be reduced.

V. Numerical Simulation

A. Key Issues for Verification and Validation

Although the algorithms are designed according to the proved lemmas and theorems, it is still necessary to verify them with concrete examples by numerical simulation. Unfortunately, each quaternion has four components, thus it is not convenient for visualization. However, it is still possible to check the algorithms proposed with the following facts:

1) the norm can be used as a necessary condition for validating the correctness of the algorithms proposed since the transition matrices $\boldsymbol{G}_\tau^{\mathbb{q}}$ are orthogonal and the norm of the quaternions should be preserved as $\|\mathbb{q}(t)\| = 1$;

2) the relation of stability, accumulative errors and time step of ESGA can be compared with other numerical methods;

3) the asymptotic behavior can be identified clearly when $\boldsymbol{\omega}(t)$ approaches to a constant vector (thus the NA-QKDE may degenerate to A-QKDE asymptotically);

4) for some special cases, we can compare the AS and NS conveniently;

5) the time complexity of ESGA and ISGA can be compared for the same NA-QKDE and configuration of parameters.

For A-QKDE, the $\boldsymbol{\omega}$ is time-invariant and $\omega = \|\boldsymbol{\omega}\|$ is a constant. Since the eigen-values of matrix $\boldsymbol{A}(\boldsymbol{\omega})$ are $\pm j\omega$, then the general solution to A-QKDE must be

$$e_i(t) = c_i \cos(\omega t + \varphi_i), \quad t \in \mathbb{R}, \quad i = 0, 1, 2, 3 \tag{33}$$

in which the amplitudes c_i and phases φ_i can be determined by the initial condition.

For NA-QKDE, if we choose the functions $\omega_2(t)$ and $\omega_3(t)$ such that for sufficient large t, $\omega_2(t) \to 0$ and $\omega_3(t) \to 0$, then (1) shows that there exists $t_* \in \mathbb{R}$ such that

$$\frac{d}{dt}\begin{bmatrix} e_0 \\ e_1 \end{bmatrix} = \begin{bmatrix} 0 & -\frac{1}{2}\omega_1 \\ \frac{1}{2}\omega_1 & 0 \end{bmatrix}\begin{bmatrix} e_0 \\ e_1 \end{bmatrix} \tag{34}$$

$$\frac{d}{dt}\begin{bmatrix} e_2 \\ e_3 \end{bmatrix} = \begin{bmatrix} 0 & \frac{1}{2}\omega_1 \\ -\frac{1}{2}\omega_1 & 0 \end{bmatrix}\begin{bmatrix} e_2 \\ e_3 \end{bmatrix} \tag{35}$$

for $t > t_*$ since $\mathbb{q} = [e_0, e_1, e_2, e_3]^T$. Hence $e_0^2(t) + e_1^2(t) = e_0^2(0) + e_1^2(0)$ and $e_2^2(t) + e_3^2(t) = e_2^2(0) + e_3^2(0)$ asymptotically. If $\omega_1(t) \to a$ asymptotically (where a is a constant), then we have

$$\frac{d^2 e_i(t)}{dt^2} + \delta_i^2 e_i(t) = 0, \quad t \geq t_*, \quad i = 0, 1, 2, 3 \tag{36}$$

where $\delta_i = a/2$. In other words, each $e_i(t)$ can be described by (33) asymptotically.

Without loss of generality, we can set the initial condition as $\mathbb{q}(0) = [1, 0, 0, 0]^T$ for the verification, thus we just need to consider $e_0(t)$ and $e_1(t)$. Let $x = \tau/2$, $\bar{t}_k = t[k] + \tau/2$, $\gamma = \omega_1(\bar{t}_k)/2$, $\boldsymbol{M} = -\gamma \boldsymbol{J}_2$, $\hat{\boldsymbol{M}} = -\boldsymbol{J}_2$ and $\tan(\theta/2) = x\gamma = \tau\omega_1(\bar{t}_k)/4$, then Lemma 2 implies that

$$\boldsymbol{G}_\tau^{e_0 e_1}(k+1|k) = \phi(x\boldsymbol{M}) = \cos\theta \boldsymbol{I}_2 - \sin\theta \boldsymbol{J}_2 \tag{37}$$

where $\theta = 2\arctan(\omega_1(\bar{t}_k)\tau/4)$. Obviously, $\boldsymbol{G}_\tau^{e_0 e_1}(k+1|k)$ is a symplectic matrix by (6).

B. Numerical Examples

We now demonstrate the intuitive ideas and show the performance of ESGA with concrete examples. All of the numerical experiments in this subsection are implemented in MATLAB and run on a desktop PC equipped with Intel® Core™ i7-3770 CPU @3.4 GHz and 4 GB RAM.

1) Numerical Solution vs. Analytical Solution: Fig. 1 illustrates the performance of ESGA-II with an AS. We set the parameters as $\omega_0 = 2\pi$, $\beta = \pi/80$, initial state $\mathbb{q}[0] = [\cos(\beta/2),\ 0, \sin(\beta/2), 0]$ and

$$\begin{aligned}\boldsymbol{\omega}(t) = [& -\omega_0(1 - \cos\beta), \\ & -\omega_0 \sin\beta \sin(\omega_0 t), \omega_0 \sin\beta \cos(\omega_0 t)]^T\end{aligned}$$

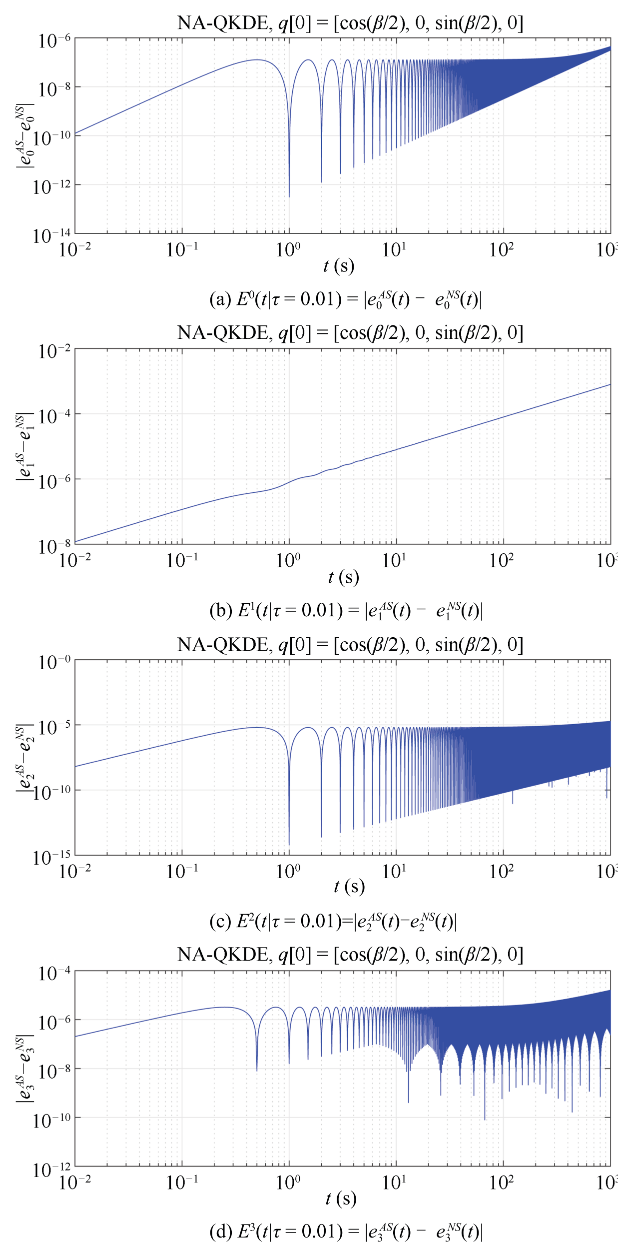

Fig. 1. Absolute errors of NS by Algorithm 2 (SGA-NA-QKDE) with $\omega_0 = 2\pi$, $\beta = \pi/80$, $\tau = 0.01\,$s, $t_0 = 0$, $t_f = 1000\,$s.

such that the AS is

$$\mathbb{q}(t) = [e_0(t), e_1(t), e_2(t), e_3(t)]^T = \left[\cos\left(\frac{\beta}{2}\right), 0, \sin\left(\frac{\beta}{2}\right)\cos(\omega_0 t), \sin\left(\frac{\beta}{2}\right)\sin(\omega_0 t)\right]^T.$$

The absolute value of error between the NS and AS for the ith component and fixed time step is defined by

$$E^i(t|\tau) = |e_i^{AS}(t) - e_i^{NS}(t)|, \quad i \in \{0, 1, 2, 3\}. \tag{38}$$

$E^i(t|\tau)$ is computed with ESGA-II for each $e_i(t)$, see Fig. 1. We find that all these errors of NS are stable and small when the time step $\tau = 0.01$ second (a low data sampling rate) and time duration is 1000 seconds. This implies that the accuracy and stability of SGA remain well for NA-QKDE.

2) Asymptotic Performance — Connection of A-QKDE and NA-QKDE: Fig. 2 demonstrates the asymptotic performance of ESGA for QKDE. We find that for different $\boldsymbol{\omega}(t)$, we have $\|\mathbb{q}(t) = 1\|$ for any t and there are no accumulated errors. On the other hand, the solutions to QKDE will have different properties for different $\boldsymbol{\omega}(t)$:

a) In Fig. 2 (a), each $e_i(t)$ is a cosine function since ω_i is a constant according to (33).

b) In Fig. 2 (b), $e_0(t)$ and $e_1(t)$ vary like cosine curves asymptotically because $\omega_1(t) \to 0$ asymptotically. Moreover, it is trivial that $e_2(t) = e_3(t) \equiv 0$ since $\omega_2(t) = \omega_3(t) \equiv 0$ and $e_2(0) = e_3(0) = 0$ by (35).

c) In Fig. 2 (c), $\omega_1(t) \to 2, \omega_2(t) \to 0, \omega_3(t) \to 0$ when $t \to \infty$. It is easy to find that each $e_i(t)$ varies periodically when $t > 10$ by (36). We remark that at $t = 0$, $\omega_2(0) \neq 0$, $\omega_3(t) \neq 0$, which leads to positive feedbacks for $e_2(t)$ and $e_3(t)$ and the increasing of their amplitudes.

d) In Fig. 2 (d), $\boldsymbol{\omega}(t)$ has no asymptotic behavior but it is periodic. Although each $e_k(t)$ varies independently, we still have $\mathbb{q}(t) \equiv 1$.

3) Stability, Accumulative Errors and Time Step: Fig. 3 shows the precision and stability with the time step. We find that the four-stage explicit Runge-Kutta (RK4) method works well only when the time step is small and the time duration is relatively short (about 15 s), otherwise the norm cannot be kept well. Furthermore, the Euler-Backward (EUB) method always leads to serious accumulative errors. Fortunately, both ESGA and ISGA work well and there is no computational damp since the norm $\|\mathbb{q}\|$ remains constant.

4) Computational Complexity — ESGA vs. ISGA (G-L Method): Fig. 4 represents the time complexity of ESGA for NA-QKDE in comparison with that of ISGA, i.e., G-L method. We solved the (1) with the same parameters $\omega(t)$ and $\mathbb{q}[0]$ as that in Fig. 1. For each fixed time step τ and component $e_i(t)$, the maximum error is defined by

$$E^i_{\max}(\tau) = \max_{t \in [t_0, t_f]} |e_i^{AS}(t) - e_i^{NS}(t)|. \tag{39}$$

The maximum errors and computing time of the two methods are calculated with different time step τ. Although the precision of ESGA is worse than that of ISGA for the same time step, the time complexity of ESGA is far lower than that of G-L method. For example, the time consumed in G-L method is about 10 times of our ESGA as shown in the figure for $\tau = 0.01$. Actually, the computing time of ESGA is almost less than 1 second for most cases in our experimental setup, however it is about 7 s for the G-L method. This implies that the ESGA is much better than ISGA if the time consumption is a key issue for hardware or software implementation. The linear time complexity $O(n)$ of our algorithms is essential for the real-time applications such as navigation and control system.

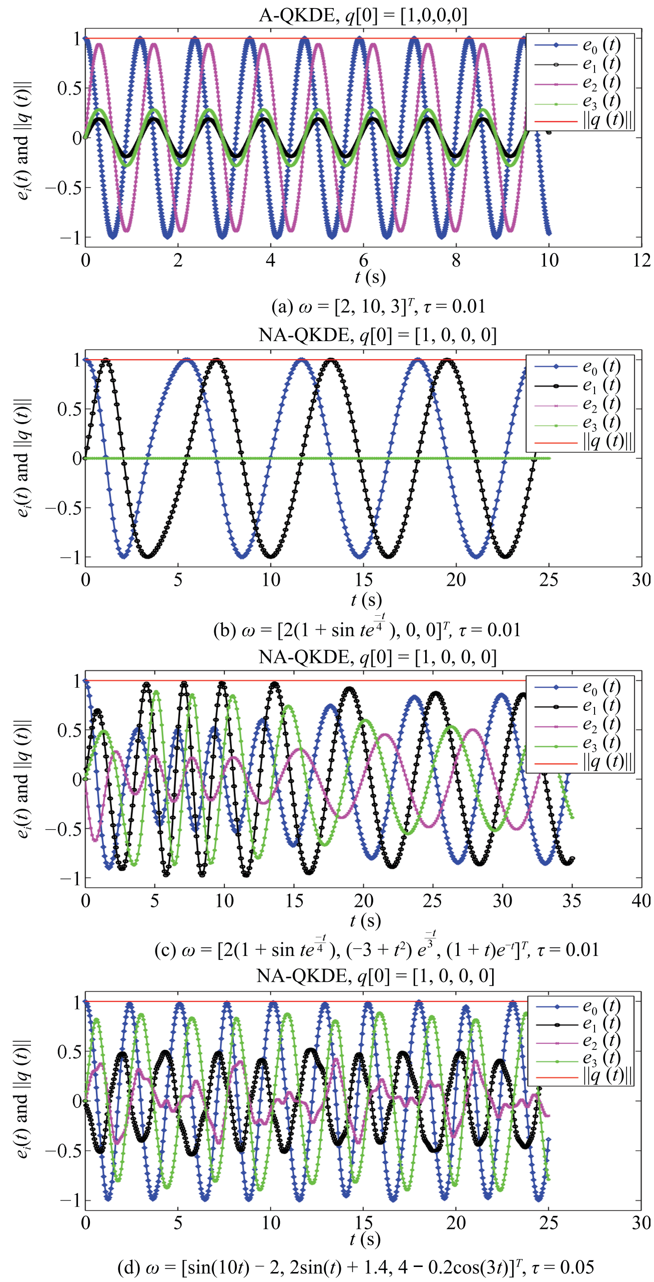

Fig. 2. NS to QKDE for different $\boldsymbol{\omega}(t)$ and $\mathbb{q}[0] = [1, 0, 0, 0]^T$.

VI. Conclusions

In this paper we proposed a key idea of solving the QKDE with symplectic method: each QKDE can be described by an autonomous or non-autonomous Hamiltonian system and the CEIS or T-CEIS can be used to design ESGA for QKDE. The generalized Euler's formula and Cayley-Euler formula for the

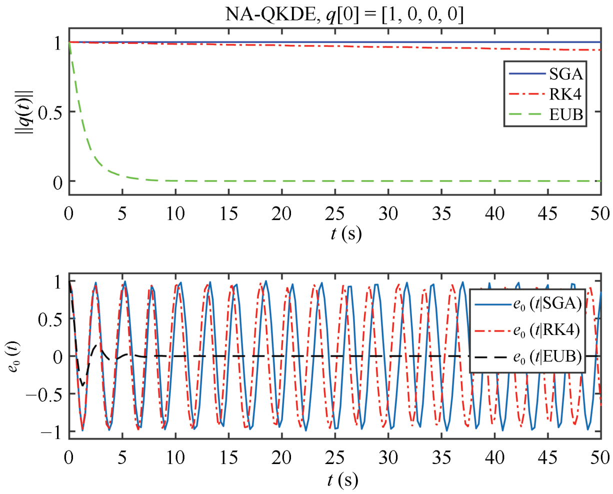

(a) Large step, $\tau = 0.25$

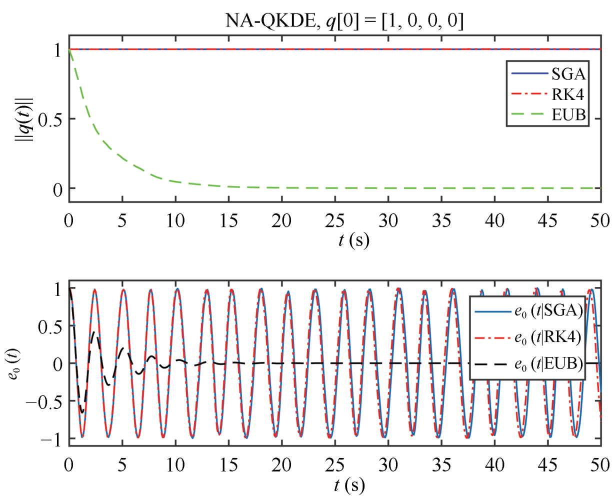

(b) Small step, $\tau = 0.10$

Fig. 3. Performances of SGA, RK4 and EUB for NA-QKDE with periodic $\boldsymbol{\omega}(t) = [\sin(10t) - 2, 2\sin(t) + 1.4, 4 - 0.2\cos(3t)]^T$.

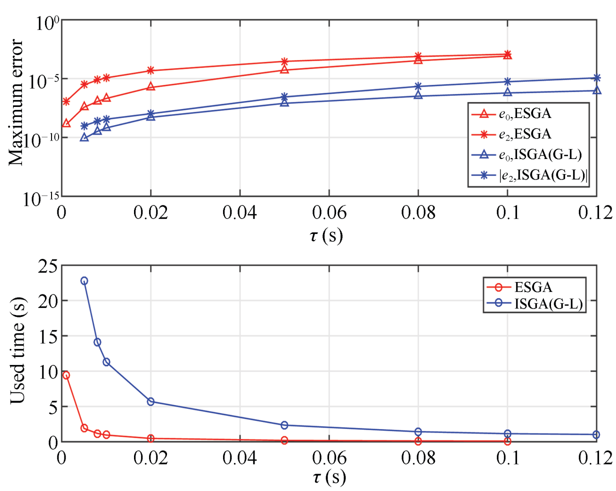

Fig. 4. Maximum errors $E^0_{\max}(\tau)$ and $E^2_{\max}(\tau)$, and computing time of ESGA-II and ISGA (G-L method) with $\omega_0 = 2\pi$, $\beta = \pi/80$, $t_0 = 0$, $t_f = 500$ s.

symplectic transition matrix play a key role in designing ESGAs with first and second order precision. The correctness and efficiencies of the ESGAs presented are verified and demonstrated by asymptotic analysis and comparison with AS and NS.

Compared with the traditional difference scheme such as RK4 and EUB, our ESGA-I for A-QKDE and EGSA-II for NA-QKDE are symplectic and can avoid the accumulative errors in the sense of long time term. On the other hand, our explicit symplectic method is better than the implicit symplectic method because of its linear time complexity and potential applications for real-time systems.

As part of future work, we will investigate the high-order precision ESGA for QKDE, the robustness of ESGA-II perturbed by noise, the applications of ESGA to more general linear time-varying system and its combination with precise-integration method. Additionally, we will also design second order precision symplectic-precise integrator to solve the linear quadratic regulator problem and the matrix Ricatti equation since they play an important role in automation.

ACKNOWLEDGMENT

The first author would like to thank Prof. Daniel Dalehaye of Ecole Nationale de l'Aviation Civile because part of this work was carried out while this author was visiting ENAC. We are indebted to Prof. Yi-Fa Tang whose lectures on symplectic geometric algorithms for Hamiltonian system at Chinese Academy of Sciences attracted the first author and stimulated this work in some sense. The authors' thanks go to Ms. Fei Liu, Mr. Jing-Tang Hao and Ms. Ya-Juan Zhang for correcting some errors in an earlier version of this paper.

REFERENCES

[1] A. C. Robinson, "On the use of quaternions in simulation of rigid-body motion," Wright Air Development Center, Tech. Rep., Dec. 1958.

[2] Y. J. Lu and G. X. Ren, "A symplectic algorithm for dynamics of rigid body," *Appl. Math. Mech.*, vol. 27, no. 1, pp. 51−57, Jan. 2006.

[3] B. Wie and P. M. Barba, "Quaternion feedback for spacecraft large angle maneuvers," *J. Guid. Contr. Dynam.*, vol. 8, no. 3, pp. 360−365, May 1985.

[4] B. Wie, H. Weiss, and A. Arapostathis, "Quarternion feedback regulator for spacecraft eigenaxis rotations," *J. Guid. Contr. Dynam.*, vol. 12, no. 3, pp. 375−380, May 1989.

[5] B. Wie and J. B. Lu, "Feedback control logic for spacecraft eigenaxis rotations under slew rate and control constraints," *J. Guid. Contr. Dynam.*, vol. 18, no. 6, pp. 1372−1379, Nov. 1995.

[6] B. Wie, D. Bailey, and C. Heiberg, "Rapid multitarget acquisition and pointing control of agile spacecraft," *J. Guid. Contr. Dynam.*, vol. 25, no. 1, pp. 96−104, Jan. 2002.

[7] J. Kuipers, *Quaternions and Rotation Sequences: A Primer with Applications to Orbits, Aerospace and Virtual Reality*. Princeton: Princeton University Press, 2002.

[8] B. Friedland, "Analysis strapdown navigation using quaternions," *IEEE Transactions on Aerospace and Electronic Systems*, vol. AES-14, no. 5, pp. 764−768, Sep. 1978.

[9] A. Kim and M. F. Golnaraghi, "A quaternion-based orientation estimation algorithm using an inertial measurement unit," in *Position Location and Navigation Symp., 2004*, Monterey, CA, USA, USA, 2004, pp. 268−272.

[10] R. Rogers, *Applied Mathematics in Integrated Navigation Systems* (third edition). Virginia, USA: AIAA, 2007.

[11] Y. M. Zhong, S. S. Gao, and W. Li, "A quaternion-based method for SINS/SAR integrated navigation system," *IEEE Trans. Aerosp. Electron. Syst.*, vol. 48, no. 1, pp. 514−524, Jan. 2012.

[12] M. Zamani, J. Trumpf, and R. Mahony, "Minimum-energy filtering for attitude estimation," *IEEE Trans. Automat. Contr.*, vol. 58, no. 11, pp. 2917−2921, Nov. 2013.

[13] J. S. Yuan, "Closed-loop manipulator control using quaternion feedback," *IEEE J. Robot. Automat.*, vol. 4, no. 4, pp. 434−440, Aug. 1988.

[14] J. Funda, R. H. Taylor, and R. P. Paul, "On homogeneous transforms, quaternions, and computational efficiency," *IEEE Trans. Robot. Automat.*, vol. 6, no. 3, pp. 382−388, Jun. 1990.

[15] J. C. K. Chou, "Quaternion kinematic and dynamic differential equations," *IEEE Trans. Robot. Automat.*, vol. 8, no. 1, pp. 53−64, Feb. 1992.

[16] O. -E. Fjellstad and T. I. Fossen, "Position and attitude tracking of AUV's: a quaternion feedback approach," *IEEE J. Oceanic Eng.*, vol. 19, no. 4, pp. 512−518, Oct. 1994.

[17] J. T. Cheng, J. Kim, Z. Y. Jiang, and W. F. Che, "Dual quaternion-based graphical SLAM," *Robot. Autonom. Syst.*, vol. 77, pp. 15−24, Mar. 2016.

[18] D. S. Alexiadis and P. Daras, "Quaternionic signal processing techniques for automatic evaluation of dance performances from MoCap data," *IEEE Trans. Multim.*, vol. 16, no. 5, pp. 1391−1406, Aug. 2014.

[19] F. Dunn and I. Parberry, *3D Math Primer for Graphics and Game Development*. Texas: WordWare Publishing Inc., 2002.

[20] D. H. Eberly, *3D Game Engine Design: A Practical Approach to Real-time Computer Graphics* (Second Edition). Boca Raton: CRC Press, 2006.

[21] J. Vince, *Quaternions for Computer Graphics*. London: Springer, 2011.

[22] T. Miller III, M. Eleftheriou, P. Pattnaik, A. Ndirango, D. Newns, and G. J. Martyna, "Symplectic quaternion scheme for biophysical molecular dynamics," *J. Chem. Phys.*, vol. 116, no. 20, pp. 8649−8659, May 2002.

[23] J. M. Cooke, M. J. Zyda, D. R. Pratt, and R. B. McGhee, "NPSNET: flight simulation dynamic modeling using quaternions," *Presence: Teleoper. Virt. Environ.*, vol. 1, no. 4, pp. 404−420, 1992.

[24] D. Allerton, *Principles of Flight Simulation*. Wiltshire, UK: John Wiley & Sons, 2009.

[25] D. J. Diston, *Computational Modelling and Simulation of Aircraft and the Environment, Volume 1: Platform Kinematics and Synthetic Environment*. Wiltshire, UK: John Wiley & Sons, 2009.

[26] J. S. Berndt, T. Peden, and D. Megginson, "JSBSim, open source flight dynamics software library," [Online]. Available: http://jsbsim.sourceforge.net/, Jan. 9, 2017.

[27] J. Hrastar, "Attitude control of a spacecraft with a strapdown inertial reference system and onboard computer," NASA, Tech. Rep., Sep. 1970.

[28] D. C. Cunningham, T. P. Gismondi, and G. W. Wilson, "Control system design of the annular suspension and pointing system," *J. Guid. Contr. Dynam.*, vol. 3, pp. 11−21, May 1980.

[29] R. B. Miller, "A new strapdown attitude algorithm," *J. Guid. Contr. Dynam.*, vol. 6, no. 4, pp. 287−291, Jul. 1983.

[30] R. A. Mayo, "Relative quaternion state transition relation," *J. Guid. Contr. Dynam.*, vol. 2, pp. 44−48, May 1979.

[31] J. C. Butcher, "Coefficients for the study of Runge-Kutta integration processes," *J. of the Australian Math. Soc.*, vol. 3, no. 2, pp. 185−201, 1963.

[32] S. J. Wang and H. Zhang, "Algebraic dynamics algorithm: Numerical comparison with Runge-Kutta algorithm and symplectic geometric algorithm," *Sci. China Ser. G: Phys. Mech. Astronom.*, vol. 50, no. 1, pp. 53−69, Feb. 2007.

[33] K. Feng, "On difference schemes and symplectic geometry," in *Proc. 1984 Beijing Symp. Differential Geometry and Differential Equations*, Beijing, China, 1984, pp. 42−58.

[34] R. D. Ruth, "A canonical integration technique," *IEEE Trans. Nuclear Sci.*, vol. 30, no. 4, pp. 2669−2671, Mar. 1983.

[35] K. Feng and M. Z. Qin, "Hamiltonian algorithms for Hamiltonian systems and a comparative numerical study," *Comput. Phys. Commun.*, vol. 65, no. 1−3, pp. 173−187, Apr. 1991.

[36] L. H. Kong, R. X. Liu, and X. H. Zheng, "A survey on symplectic and multi-symplectic algorithms," *Appl. Math. Comput.*, vol. 186, no. 1, pp. 670−684, Mar. 2007.

[37] K. Feng and M. Z. Qin, *Symplectic Geometric Algorithms for Hamiltonian systems*. Berlin Heidelberg: Springer, 2010.

[38] J. M. Sanz-Serna and M. P. Calvo, *Numerical Hamiltonian problems*. London: Chapman and Hall/CRC, 1994.

[39] E. Hairer, C. Lubich, and G. Wanner, *Geometric Numerical Integration: Structure-Preserving Algorithms for Ordinary Differential Equations*. Berlin Heidelberg: Springer, 2006.

[40] J. C. Butcher, "Implicit Runge-Kutta processes," *Math. Comput.*, vol. 18, no. 85, pp. 50−64, Jan. 1964.

[41] A. Iserles, *A First Course in the Numerical Analysis of Differential Equations*. Cambridge: Cambridge University Press, 1996.

[42] J. M. Varah, "On the efficient implementation of implicit Runge-Kutta methods," *Math. Comput.*, vol. 33, no. 146, pp. 557−561, 1979.

[43] V. I. Arnold, *Mathematical Methods of Classical Mechanics*. New York: Springer, 1989.

[44] V. I. Arnold, V. V. Kozlov, and A. I. Neishtadt, *Mathematical Aspects of Classical and Celestial Mechanics*. Berlin Heidelberg: Springer, 2006.

[45] L. H. Kong, J. L. Hong, L. Wang, and F. F. Fu, "Symplectic integrator for nonlinear high order Schrödinger equation with a trapped term," *J. Comput. Appl. Math.*, vol. 231, no. 2, pp. 664−679, Sep. 2009.

[46] J. Franco and I. Gómez, "Construction of explicit symmetric and symplectic methods of Runge-Kutta-Nyström type for solving perturbed oscillators," *Appl. Math. Comput.*, vol. 219, no. 9, pp. 4637−4649, Jan. 2013.

[47] D. M. Hernandez, "Fast and reliable symplectic integration for planetary system *N*-body problems," *Mon. Not. R. Astronom. Soc.*, vol. 458, no. 4, pp. 4285−4296, Jun. 2016.

[48] V. Guillemin and S. Sternberg, *Symplectic Techniques in Physics*. Cambridge: Cambridge University Press, 1990.

[49] S. Sternberg and Y. Li, *Lectures on Symplectic Geometry*. Tsinghua University Press, 2012.

[50] A. C. da Silva, *Lectures on Symplectic Geometry*. Berlin Heidelberg: Springer, 2008.

Hong-Yan Zhang received the B.S. and M.S. degrees in applied physics and telecommunication engineering in 2000 and 2003 from Xidian University, China. He received the Ph.D. degree in 2011 from the Institute of Automation, Chinese Academy of Science. Currently, he is with the School of Information Science and Technology, Hainan Normal University, China. His research interests include applied mathematics, computer vision, and non-destructive testing.

Zi-Hao Wang received the B.S. degree in aviation engineering in 2015 from Civil Aviation University of China (CAUC). He is now a graduate student of Sino-European Institute of Aviation Engineering (SIAE), CAUC. His research interests include applied mathematics, computer vision, machine learning, and aviation engineering.

Lu-Sha Zhou received the B.S. degree in aviation engineering in 2014 from Civil Aviation University of China (CAUC). She is now a graduate student of Sino-European Institute of Aviation Engineering (SIAE), CAUC. Her research interests include applied mathematics, computer vision, robotics and their applications in aviation engineering.

Qian-Nan Xue received the Ph.D. degree in 2012 from the Institute of Electronics, Chinese Academy of Sciences. Currently, she is with Tianjin Key Laboratory for Civil Aircraft Airworthiness and Maintenance, Civil Aviation University of China. Her research interests include circuit design, sensors and non-destructive testing.

Long Ma received the B.S. and Ph.D. degrees in measurement technology and instruments in 2006 and 2011 from Tianjin University, China. Currently, he is with the Sino-European Institute of Aviation Engineering (SIAE), Civil Aviation University of China. His research interests include sensors, navigation system, computer vision, and non-destructive testing.

Yi-Fan Niu received the M.S. and Ph.D. degrees in materials science in 2005 and 2009 from the University of Rennes 1, France. Currently, she is with the Sino-European Institute of Aviation Engineering (SIAE), Civil Aviation University of China. Her research interests include micro-lenz design and its applications in optics, composite materials, and system modelling.